International Journal of Impact Engineering 46 (2012) 56–61

Contents lists available at SciVerse ScienceDirect

International Journal of Impact Engineering

journal homepage: www.elsevier.com/locate/ijimpeng

Short communication

Shock testing accelerometers with a Hopkinson pressure bar

J.T. Foster [a,*], D.J. Frew [b], M.J. Forrestal [c], E.E. Nishida [d], W. Chen [e]

[a] The University of Texas at San Antonio, One UTSA Circle, San Antonio, TX 78249, USA
[b] Dynamic Systems and Research, Inc., 8219 Pickard Ave. NE, Albuquerque, NM 87110, USA
[c] Consultant, 1805 Newton Pl. NE, Albuquerque, NM 87106, USA
[d] Sandia National Laboratories, P.O. Box 5800, Albuquerque, NM 87185-1160, USA
[e] Purdue University, 3323 Neil Armstrong Hall of Engineering, 701 W. Stadium Ave., West Lafayette, IN 47907, USA

ARTICLE INFO

Article history:
Received 8 July 2011
Received in revised form
2 February 2012
Accepted 14 February 2012
Available online 22 February 2012

Keywords:
Shock testing accelerometers
Hopkinson pressure bar
Pulse shaping

ABSTRACT

The electronic industry continues to dramatically reduce the size of electrical components. Many of these components are now small enough to allow shock testing with Hopkinson pressure bar techniques. However, conventional Hopkinson bar techniques must be modified to provide a broad array of shock pulse amplitudes and durations. For this study, we evaluate the shock response of accelerometers that measure large amplitude pulses, such as those experienced in projectile perforation and penetration tests. In particular, we modified the conventional Hopkinson bar apparatus to produce relatively long duration pulses. The modified apparatus consists of a steel striker bar, annealed copper pulse shapers, an aluminum incident bar, and a tungsten disk with mounted accelerometers. With these modifications, we obtained accelerations pulses that reached amplitudes of 10 kG and durations of 0.5 ms. To evaluate the performance of the accelerometers, acceleration-time responses are compared with a model that uses data from a quartz stress gage. Comparisons of data from both measurements are in good agreement.

© 2012 Elsevier Ltd. All rights reserved.

1. Introduction

A major goal for our penetration technology program is to obtain a fundamental understanding of the penetration process for concrete targets. For many applications [1,2], the projectile nose does not erode and the projectile has relatively small deformations. In those cases, rigid-body deceleration data from data recorders mounted within the projectile provide a close measure of net force on the projectile nose. Because tests with projectiles that are large enough to contain an acceleration data recorder are expensive, it seems prudent to conduct inexpensive performance evaluation experiments on the accelerometers prior to penetration tests. As pointed by Togami et al. [3], there are no standard calibration methods for high-G accelerometers, so performance evaluation prior to penetration tests adds to the confidence of the penetration data.

In a previous study [4], we presented a Hopkinson bar technique to examine the performance of accelerometers and reported durations to about 0.1 ms. In this study, we make modifications to the apparatus in [4] and report durations to about 0.5 ms. In particular, we use a longer steel striker bar and two annealed copper pulse shapers. Experimental details are explained in the next section. Next, we present models that predict the incident strain pulse and the acceleration response of the tungsten disk and mounted accelerometers. We conclude with a comparison of the measured acceleration and a model that predict acceleration from data taken with a quartz stress gage. Comparisons of data from both measurements show good agreement.

2. Experimental apparatus and procedure

Figs. 1 and 2 show the modified Hopkinson bar apparatus. A maraging steel (C350) striker bar impacts the double, annealed copper (C11000) pulse shaper that is attached to the 7075-T651 aluminum incident bar. The pulse shaper produces a nondispersive, compressive stress wave that propagates in the aluminum incident bar and eventually interacts with the tungsten disk at the end of the bar. Strain gages are attached to the incident bar [5], a quartz stress gage [6] is placed between the end of the incident bar and the disk, and two accelerometers [7,8] from different suppliers are mounted to the end of the disk. In a previous study [4], we reported acceleration–time durations of about 0.1 ms. To achieve durations of about 0.5 ms, we use a longer ($L = 0.610$ m) steel striker bar and the double pulse shaper [9,10] shown in Fig. 2. The disk is attached to the incident bar with a plastic shrink tube that allows the disk to

* Corresponding author. +1 2104585521.
E-mail address: john.foster@utsa.edu (J.T. Foster).

0734-743X/$ – see front matter © 2012 Elsevier Ltd. All rights reserved.
doi:10.1016/j.ijimpeng.2012.02.006

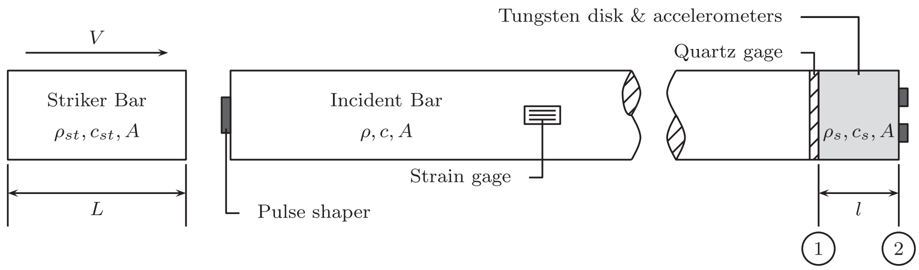

Fig. 1. Schematic of modified Hopkinson apparatus.

separate from the incident bar when the interface stress becomes tensile. Thus, we achieve a single pulse loading.

We now have several analytical models that help us design our experiments without many unnecessary experimental trials. In [9,10], we presented models that predict incident stress pulses for single and double pulse shapers. We show in the next sections that predictions and measured incident strain pulses are in good agreement. Next we performed a stress wave analysis in the tungsten disk [4] and show that rise time of the incident stress pulse is long enough and the tungsten disk length is short enough that the disk response can accurately be approximated as rigid-body motion. Since we measure stress at the aluminum bar-tungsten disk interface with the quartz gage, we can calculate rigid-body acceleration of the tungsten disk from Newton's Second Law and the stress gage data. Thus, we have an independent comparison with the measured acceleration-time pulse.

The experimentally verified model for the rigid-body acceleration of the disk shows that the shapes of the acceleration–time pulses are dominated by the slopes of the incident stress wave. Thus, shaping the incident stress with the pulse shaper shown in Fig. 2 is a critical item for this modified Hopkinson bar technique. We use the high impedance tungsten disk, so that the incident bar-disk interface remains in compression with multiple wave transits in the disk.

3. Incident stress without pulse shaper

Fig. 1 shows the Hopkinson bar apparatus. We eliminate the pulse shaper and study the incident pulse for a steel striker bar and an aluminum incident bar. For this bar combination, the stress at the bar interface remains in compression during multiple reflections in the striker and lengthens the incident pulse duration. In this section, we present a model and data that demonstrate this effect.

For the analysis, we use the notation in Fig. 1 and the elementary theory for wave propagation in bars [11]. The striker bar moves to the right at constant velocity V, so all the particles in the striker bar have particle velocity $\upsilon = V$. After impact, compression stresses travel in both bars. For bars of equal area, the reflected stress in the striker bar is equal to the transmitted stress in the incident bars, so

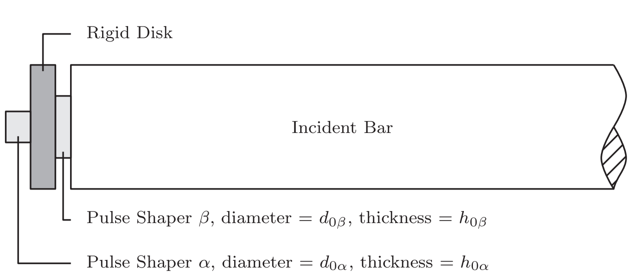

Fig. 2. Schematic of pulse shaper design.

$$\sigma_r = \sigma_i \tag{1}$$

where stress is measured positive in compression. The bars remain in contact, and the particle velocities at the interface are equal, so

$$V - \upsilon_r = \upsilon_i \tag{2}$$

where υ_r is the reflected and υ_i is the transmitted particle velocity measured positive to the right. For the notation in Fig. 1,

$$\sigma_r = \rho_{st} c_{st} \upsilon_r, \quad \sigma_i = \rho c \upsilon_i \tag{3}$$

With Eqs. (1)–(3), we obtain

$$\sigma_r = \rho_{st} c_{st} V \left(\frac{r}{1+r}\right) \tag{4a}$$

$$\sigma_i = \frac{\rho c V}{1+r} \tag{4b}$$

$$r = \frac{\rho c}{\rho_{st} c_{st}} \tag{4c}$$

Eqs. (4a)–(4c) are valid until the tensile wave that reflects from the free end of the striker reaches the striker–incident bar interface. We define

$$\tau = \frac{2L}{c_{st}} \tag{5}$$

so Eqs. (4a)–(4c) are valid for $0 < t < \tau$.

At $t = \tau/2$, the left traveling compression wave in the striker reaches the free end and reflects as a right traveling tensile wave. When $t = \tau$, this tensile wave reaches the striker–incident bar interface. Now, let σ_r', σ_i' be the reflected and transmitted compression waves that result from the right traveling tensile wave that reaches the interface. For bars of equal area

$$\sigma_r - \sigma_r + \sigma_r' = \sigma_i + \sigma_i' \tag{6}$$

From Eqs. (1) and (6)

$$\sigma_r' = \sigma_i' + \sigma_r \tag{7}$$

where σ_r is given by Eq. (4a). Particle velocity continuity at the interface requires that

$$V - \upsilon_r - \upsilon_r - \upsilon_r' = \upsilon_i + \upsilon_i' \tag{8}$$

From Eq. (2), $V - \upsilon_r = \upsilon_i$ and

$$\upsilon_r' = -\upsilon_i' - \upsilon_r \tag{9}$$

where υ_r is given by Eqs. (3) and (4a). For the notation in Fig. 1,

$$\sigma_r' = \rho_{st} c_{st} \upsilon_r', \quad \sigma_i' = \rho c \upsilon_i' \tag{10}$$

With Eqs. (7), (9), and (10),

Download English Version:

https://daneshyari.com/en/article/776823

Download Persian Version:

https://daneshyari.com/article/776823

Daneshyari.com